Object Kinetic Monte Carlo calculations of irradiated Fe–Cr dilute alloys: The effect of the interaction radius between substitutional Cr and self-interstitial Fe

L. Gámez [a], B. Gámez [a], M.J. Caturla [b,*], D. Terentyev [c], J.M. Perlado [a]

[a] Instituto de Fusión, Universidad Politécnica de Madrid, Belgium
[b] Departamento de Física Aplicada, Universidad de Alicante, Alicante E-03690, Spain
[c] SCK-CEN, Mol, Belgium

Keywords:
Monte Carlo simulations
FeCr alloys
Radiation effects
Fusion materials
Fission materials

A B S T R A C T

Object Kinetic Monte Carlo models allow for the study of the evolution of the damage created by irradiation to time scales that are comparable to those achieved experimentally. Therefore, the essential Object Kinetic Monte Carlo parameters can be validated through comparison with experiments. However, this validation is not trivial since a large number of parameters is necessary, including migration energies of point defects and their clusters, binding energies of point defects in clusters, as well as the interaction radii. This is particularly cumbersome when describing an alloy, such as the Fe–Cr system, which is of interest for fusion energy applications. In this work we describe an Object Kinetic Monte Carlo model for Fe–Cr alloys in the dilute limit. The parameters used in the model come either from density functional theory calculations or from empirical interatomic potentials. This model is used to reproduce isochronal resistivity recovery experiments of electron irradiated dilute Fe–Cr alloys performed by Abe and Kuramoto. The comparison between the calculated results and the experiments reveal that an important parameter is the capture radius between substitutional Cr and self-interstitial Fe atoms. A parametric study is presented on the effect of the capture radius on the simulated recovery curves.

1. Introduction

Development of optimal materials for fusion applications and next generation fission reactors can greatly benefit from the use of reliable models capable of describing the production and evolution of lattice defects. These models can be used to limit the number of experiments performed to test these materials, and, up to some extent, to extrapolate the available experimental data, since the range of parameters to consider (fluence, flux, temperature, alloy composition, etc.) is extremely large. Recently, multi-scale modeling has been advancing in the direction of building validated models starting from first principles calculations (see for example [1,2]).

Ferritic/martensitic steels are considered as good candidates for structural materials in both fusion and generation IV reactors [3,4]. The Cr concentration considered in these materials is in the range of a few at.% (7–17 at.% of Cr). In this work we present an Object Kinetic Monte Carlo approach (OKMC) to study damage accumulation and evolution in Fe–Cr alloys with input from recently published density functional theory (DFT) and empirical potential calculations. As a first test of the model being developed for Fe–Cr alloys, we consider low Cr concentrations, below 1 at.% of Cr, for which systematic experiments addressing the mobility of point defects have been performed in the past [5].

2. Model

In order to model the recovery of the resistivity during annealing measured experimentally in electron irradiated Fe and dilute Fe–Cr alloys, we use an OKMC approach. The OKMC method is based on the residence time algorithm [6] and it has been explained extensively elsewhere (see for example Refs. [7,8]). Briefly, this method follows the evolution in time of defects and defect clusters, resolving their positions in 3D space. The information necessary to evolve the system is the migration energy of each type of defect as well as the dissociation energy for each cluster of defects, and the barrier for the defect formation in case it exists. This information is usually taken from DFT calculations or simulations using empirical interatomic potentials. For the purpose of this article, it is important to point out that another parameter in these simulations is the capture radius considered for the interaction between different defects to form clusters. The interaction between two defects occurs when their distance is equal or smaller than the capture radius.

The OKMC algorithm computes the rate of each possible event in the simulation. The events are (i) the diffusive jump of a defect, (ii) the dissociation of a defect from a cluster and (iii) the

* Corresponding author.
E-mail address: mj.caturla@ua.es (M.J. Caturla).

introduction of a new defect or a cluster of defects (a cascade) due to the irradiation. The rate for events of type (i) and (ii) are calculated from the defect migration and dissociation energies, respectively. The rate of introduction of a new cascade is given by the dose rate of the experiment being simulated. The total rate for each event is the product of the rate of the event and the number of objects in the simulation setup that can perform that event. The total rate for each simulation step is the sum of these terms for all possible events. At each OKMC step an event is selected randomly from the total rate, and the simulation time, obtained from the inverse of the total rate, is updated. For more information about the OKMC algorithm see Refs. [7,8].

In the calculations presented here the type of defects considered are Fe self-interstitials (I) and their clusters (I_n where n is the number of Fe atoms in the cluster), vacancies (V) and vacancy clusters (V_n), Cr atoms in substitutional positions (Cr), and mixed (i.e. Fe–Cr dumbbells) self-interstitials (ICr). Clusters of mixed self-interstitials are also considered up to size two. These clusters are I_2Cr (i.e. the cluster contains two dumbbells, one Fe–Fe and one Fe–Cr) and I_2Cr_2 (with two Fe–Cr dumbbells). In addition, we also consider the formation of the immobile configuration ICr_2 due to the trapping of the ICr by substitutional Cr atoms. Higher order clusters or trapping configurations are not considered in the present calculations.

Table 1 shows the migration energies of the defects considered in the calculations. Self-interstitials and vacancies up to size four are mobile while clusters of a larger size are treated as immobile in these simulations, as is done in previous kinetic Monte Carlo models for pure Fe [11]. The mixed self-interstitial (ICr) is also mobile and note that its migration energy is lower than for the Fe self-interstitial (I), according to the calculations done using empirical potentials and DFT [9,10]. Clusters can also emit defects with a dissociation barrier given as the sum of the corresponding binding energy of the defect to the cluster plus the migration energy of the defect that is emitted. The values of binding energies, migration energies and dissociation energies used in these calculations are summarized in Table 2, together with the corresponding references.

Considering the information about defect energetics described above, we have simulated the evolution of those defects produced under the experimental conditions described in Ref. [5]. In these experiments, pure Fe and dilute Fe–Cr alloys were irradiated with 1 MeV electrons at 77 K and then isochronally annealed to measure the recovery of electrical resistivity. To simulate these experiments an OKMC box size of 287 nm × 287 nm × 287 nm was used with periodic boundary conditions and no sinks such as dislocations or grain boundaries, conditions previously used by Fu et al. to simulate the recovery of the resistivity in electron irradiated Fe [11]. In the case of the Fe–Cr alloys, we have performed simulations for three

Table 1
Migration energies of defects used in the OKMC simulations.

Species	Migration energy (eV)	Reference
I	0.34	[11]
I_2	0.43	[11]
I_3	0.43	[11]
I_4	0.40	*
I_5 and up	Immobile	
V	0.67	[11]
V_2	0.62	[11]
V_3	0.35	[11]
V_4	0.48	[11]
V_5 and up	Immobile	
ICr	0.23	[9]
I_2Cr	0.30	[15]
All other I_nCr_m clusters	Immobile	

* This value was assumed based on the values for smaller interstitial clusters.

Table 2
Dissociation energies of defects used in the OKMC simulations. Values of binding energies and migration energies with their corresponding references.

Species	Dissociation reaction	Binding energy (eV) and reference		Dissociation energy (eV)
ICr	Cr + I	0.08	[15,16]	0.42
ICr_2	Cr + ICr	0.08	[15,16]	0.31
ICr_2	Cr_2 + I	0.39	[15,16]	0.73
I_2Cr	ICr + I	0.65	[15,16]	0.88
I_2Cr	Cr + I_2	0.02	[15,16]	0.45
I_2Cr_2	Cr + I_2Cr	0.06	[15,16]	0.36
I_2Cr_2	Cr_2 + I_2	0.32	[15,16]	0.75
I_2Cr_2	ICr + ICr	0.63	[15,16]	0.86
I_2Cr_2	ICr_2 + I	0.63	[15,16]	0.97
I2	I + I	0.8	[11]	1.14
I3	I2 + I	0.92	[11]	1.26
I4	I3 + I	1.64	[11]	1.98
In ($n > 4$)	In-1 + I	*	[11]	
V2	V2 + V	0.30	[11]	0.97
V3	V3 + V	0.37	[11]	1.04
V4	V4 + V	0.62	[11]	1.29
Vn	Vn-1 + V	*	[11]	

* Extrapolation law as described in [11].

Table 3
Initial concentration of Frenkel pairs used in the OKMC calculations for the experimental conditions of [5], calculated considering a Frenkel-pair resistivity of 30 μΩ cm/at.% [5,12].

Cr concentration	Initial resistivity from [5]	Number of Frenkel-pairs in the OKMC model
Pure Fe (Cr = 0)	71.2 nΩ cm/at.%	24000 (24 appm)
FeCr 0.019 at.%	80.5 nΩ cm/at.%	27000 (27 appm)
FeCr 0.047 at.%	72.6 nΩ cm/at.%	24000 (24 appm)
FeCr 0.095 at.%	140 nΩ cm/at.%	47000 (47 appm)

different values of the initial Cr concentration, corresponding to those used in the experiments: 0.019 at.%, 0.047 at.% and 0.095 at.% [5]. Substitutional Cr is distributed randomly in the simulation box with the appropriate ratio for each concentration. Regarding the initial distribution of Frenkel pairs created by the electron irradiation, we have taken into account that the initial resistivity values given in [5] are different for each material. Table 3 shows the values of the initial resistivity as given by Abe and Kuramoto [5] and the corresponding initial number of Frenkel pairs used in the calculations. In order to obtain the initial concentration of Frenkel pairs we have used a value of resistivity per Frenkel pair of 30 μΩ cm/at.% corresponding to pure Fe [5,12]. However this is not appropriate when considering concentrated Fe–Cr alloys due to departure of the Matthiessen's rule [12]. The Frenkel-pairs are also distributed randomly in the simulation box.

An isochronal annealing with a temperature step of 3 K and a time step of 3 min, as in the experiments [5], is performed. The total number of defects as a function of temperature is related to the resistivity recovery curves obtained experimentally. In the experiments of [5] the resistivity change has been renormalized to the initial resistivity value after the electron irradiation, therefore, in order to compare, the total number of defects has also been renormalized to the initial number of defects in the simulation. The derivative of these curves with temperature can then be compared to the experimental data presented in [5].

3. Results

Fig. 1 shows the evolution of the derivative of the number of defects during the annealing, normalized to the initial number of defects after irradiation, as obtained from the OKMC calculations performed in: pure Fe, 0.019 at.% Cr, 0.047 at.% Cr and 0.095 at.% Cr.

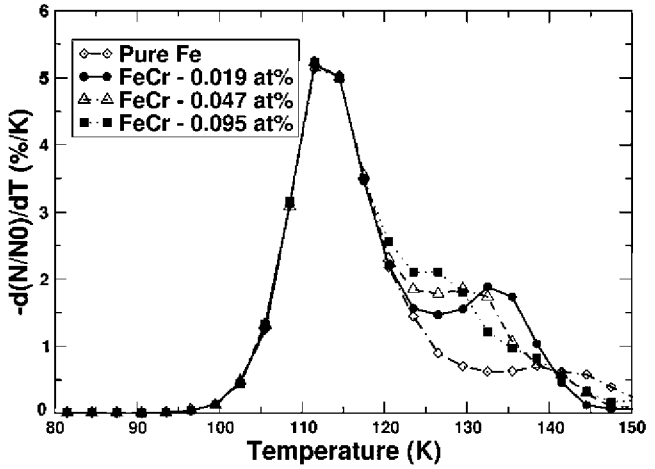

Fig. 1. Derivative with temperature of the total number of defects (normalized to the initial number after irradiation) as a function of temperature for the case of pure Fe and three different Fe–Cr alloys.

In the temperature range of 80–150 K two peaks are observed, as already described with event kinetic Monte Carlo by Fu et al. for the case of pure Fe [11]. The first peak, named I_{D2} [13], corresponds to the correlated recombination of I and V pairs belonging to the same Frenkel pair. The second peak, named I_E, is attributed to the recombination between I and V due to the long range migration of I. Note that in the case of pure Fe, the I_E stage, located at around 140 K, has a much smaller amplitude than that of the I_{D2} stage.

The main effect that can be observed in the presence of Cr is the shift of the I_E peak towards lower temperature as the Cr concentration increases, just as observed experimentally [5,14]. The reason for this shift is the formation of ICr defects which have lower migration energy than Fe–Fe self-interstitials (0.23 vs. 0.34 eV). The ICr, however, also has a low dissociation energy (0.42 eV), yet it performs several jumps prior to the dissociation, and therefore may recombine with vacancies which are immobile up to about 220 K (given that their migration energy is about 0.6 eV).

The shift of the I_E stage with Cr concentration has also been reproduced by rate theory calculations [15] using similar defect energetics as those presented here, although with different initial conditions. In the case of rate theory, the I_{D2} stage is not obtained since its reproduction requires the spatial correlations to be included in a mean field approach.

In order to further understand the effect of Cr on defect evolution, we present in Fig. 2 the number of defects, normalized to the initial number after irradiation, as a function of temperature for the case of pure Fe (Fig. 2(a)) and Fe-0.047 at.% of Cr (Fig. 2(b)). We have selected this particular Cr concentration for the comparison since the initial number of defects is the same as in the case of pure Fe, (see Table 3), so that the differences cannot be attributed to a dose effect. In Fig. 2(b), only pure Fe defects are included for clarity.

The most significant difference that can be observed for these two conditions is the higher recombination between vacancies and self-interstitials occurring in the presence of Cr. In the case of pure Fe, 83% of the defects have recombined at a temperature of 150 K and only 17% of the defects remain, while for the case of 0.047 at.% of Cr, 94% of the defects produced by the irradiation have recombined at this same temperature. As can be observed in Fig. 2(a), in pure Fe at 150 K defects are mainly single vacancies and self-interstitials in small clusters, mostly of size 2 and 3, but self-interstitial clusters of size 4 and higher also exist. In the case of Fig. 2(b), the remaining defects at this temperature are also mostly single vacancies and clusters with two self-interstitials

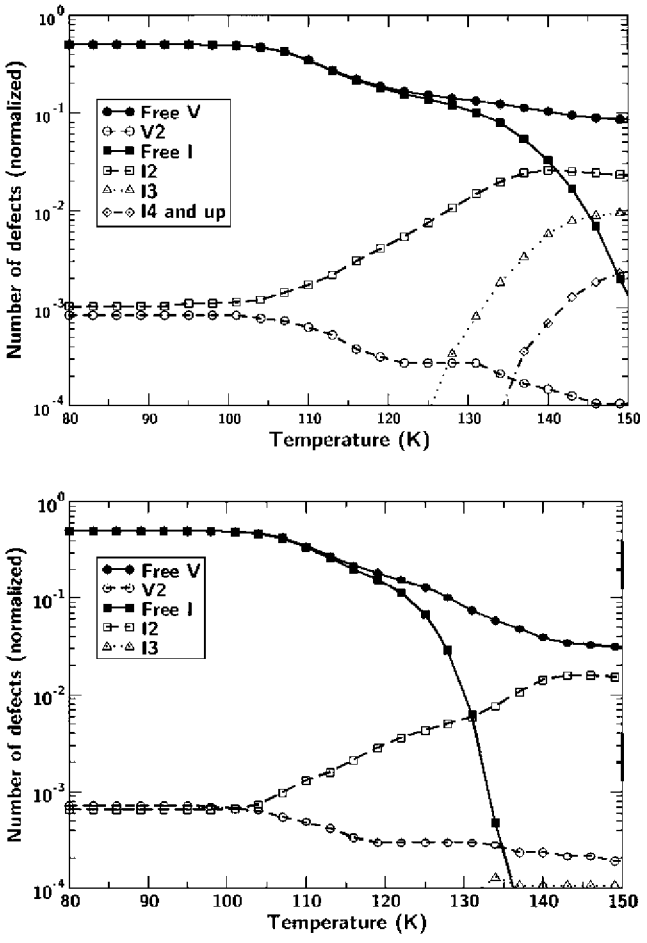

Fig. 2. Evolution of the concentration of defects versus temperature (normalized to the initial number of defects after irradiation) for (a) pure Fe and for (b) a Fe–Cr alloy with 0.047 at.% Cr. In Fig. 2(b) only pure Fe self-interstitials are shown for comparison.

(I_2) but the concentration of I_3 clusters is very low and no higher order interstitial clusters are present at this temperature.

For the case of the Fe–Cr alloy we also have to take into account the evolution of mixed clusters, I_nCr_m, as a function of temperature. This is shown in Fig. 3 for the same case as in Fig. 2(b) 0.047 at.% of Cr. The concentration of the ICr complexes is always very low, but one must keep in mind that these defects have both low migration and dissociation energies. As a result, they form by the interaction of I and substitutional Cr, but they also migrate at low temperatures (their migration energy is only 0.23 eV), and therefore recombine with immobile vacancies or form higher order clusters. In fact ICr can recombine with vacancies leaving a substitutional Cr which will contribute to the enhanced defect recombination observed in the presence of Cr. Since the dissociation energy of ICr is also very low (0.42 eV) it can also emit an Fe–Fe self-interstitial leaving a substitutional Cr atom. Consequently, the ICr defects constantly form, dissociate and interact with other defects.

Besides vacancy recombination, ICr can also form other complexes. It can interact with another ICr forming I_2Cr_2, with substitutional Cr forming ICr_2 or with Fe–Fe self-interstitials forming an I_2Cr, as can also be observed in Fig. 3. In the case of I_2Cr, since it is also considered as mobile, it again contributes to a higher recombination than in pure Fe. Note, however, that all these clusters disappear at ~150 K due to their low dissociation energy. The I_2Cr complex dissociates through the emission of an I_2 self-interstitial cluster, which explains the increase in the number of I_2 self-inter-

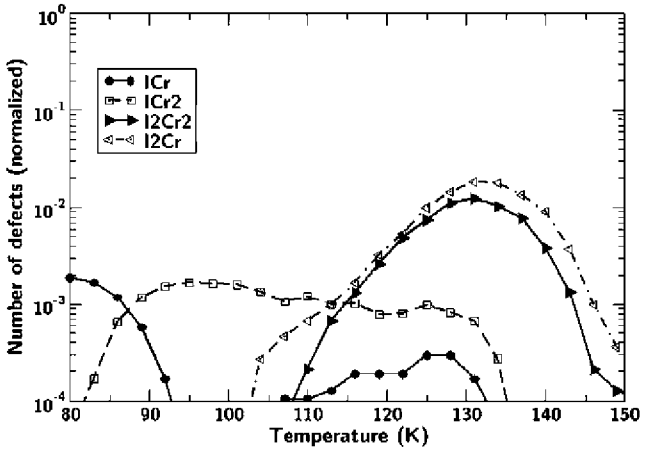

Fig. 3. Evolution of the concentration of I_mCr_n complexes versus temperature for an Fe–Cr alloy with 0.047 at.% of Cr.

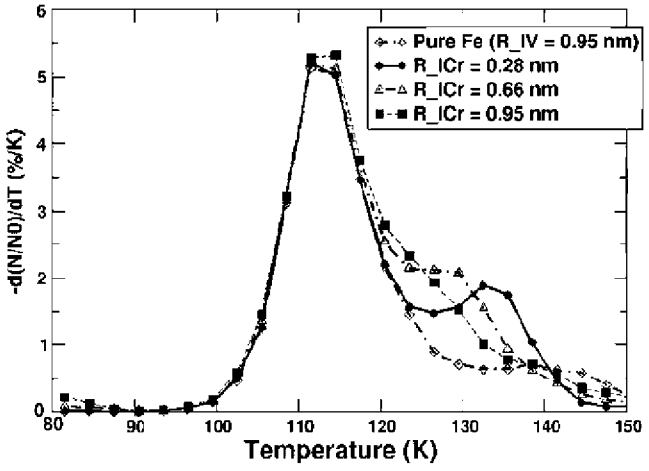

Fig. 4. Dependence of the position and shape of the I_E peak on I-Cr capture radius, calculated for a Fe–Cr alloy with 0.019 at.% of Cr.

stitials observed at around 130 K in Fig. 2(b), which is the temperature at which the total number of I_2Cr complexes starts decreasing (see Fig. 3). As a result, the total number of I_2 at 150 K both in pure Fe and the particular Cr concentration described here, are similar.

As shown in Fig. 1, higher Cr concentrations lead to a higher number of ICr and therefore a stronger shift in the I_E peak. The concentration of ICr is, consequently, an important parameter. In turn, the rate of formation of ICr is determined by the concentration of substitutional Cr and I, by the mobility of I and also by the capture radius ($R_{\_ICr}$) considered for the interaction between I and Cr. The concentration of substitutional Cr and Fe–Fe self-interstitials are given by the particular conditions of the experiment, the alloy composition and the irradiation dose respectively. For the particular experimental conditions considered here, the concentration of Cr exceeds that of defects produced by the irradiation. For example, for the lowest Cr concentration case, 0.019 at.%, the initial number of defects is 0.0012%, as can be calculated from the number of Frenkel pairs in Table 2. As a result, a large number of ICr complexes is expected to form, and the capture radius used for the interaction between self-interstitials and Cr will have an important effect. For the case of pure Fe, a capture radius between a self-interstitial and a vacancy of 0.95 nm ($3.3a_0$, where a_0 is the lattice parameter of α-Fe) was used following reference [11]. Using this value the position of the I_{D2} peak in pure Fe obtained from the simulations coincides with that measured experimentally. The effect of $R_{\_ICr}$ on the position of the I_E peak has been evaluated by varying $R_{\_ICr}$ while keeping all other parameters in the simulation constant.

Fig. 4 shows the derivative with temperature of the normalized defect concentration as a function of temperature for the case of 0.019 at.% Cr and for $R_{\_ICr}$ equal to 0.95 nm ($3.3a_0$), 0.66 nm ($2.3a_0$) and 0.28 nm ($1.0a_0$). The case of pure Fe is also included for comparison. It is interesting to note that if $R_{\_ICr}$ is taken as $R_{\_IV}$ (i.e. $3.3a_0$), the I_E peak almost disappears by merging with the I_{D2} peak, contrary to what is observed experimentally. This effect is even more pronounced when calculations are performed for higher Cr concentrations (not shown here). The best agreement obtained with respect to the experimental observations is for a capture radius of 0.28 nm which corresponds to the radius of a second neighbour shell, and is the value used for the calculations reported in Fig. 1. This result indicates that the interaction between I and Cr is essentially of the short range type, unlike in the case of a self-interstitial and vacancy. Moreover, DFT calculations show that the sign of the interaction depends on the specific position of a substitutional Cr and spatial orientation of the ⟨110⟩ Fe–Fe dumbbell, so that there is a number of sites where the interaction is attractive and others where it is repulsive [16,17]. Hence, the actual interaction range is larger than the value of a_0 obtained in these calculations, but not all pairs of I and Cr within the interaction range will be oriented such that an attractive interaction would occur. Given that in these particular OKMC calculations the orientation of I is not taken into account, the obtained capture radius can be interpreted as an effective value, smaller than the actual interaction range, to account for the configurations with repulsive interactions. Nevertheless, validation of the capture radius by other means, such as atomistic simulations or experiments would be desirable since it plays an important role in the defect evolution, especially at higher temperatures. For example, although it not shown here for lack of space, if one sets $R_{\_ICr}$ as $3.3a_0$, the experimentally observed peak in the resistivity recovery at 180 K [5] cannot be reproduced.

As can be seen from the results presented above, in a complex system such as an alloy, even in the dilute limit, the number of reactions included in the OKMC calculations is quite large. Ideally, we would like to have a model with the minimum number of interactions that is capable of reproducing different experimental conditions. However, often understanding the importance of a particular reaction is not obvious from the results of a simulation. In the model proposed in this work I_nCr_m clusters can grow up to size $n = m = 2$. We have seen that the formation of I_2Cr clusters occurs at low temperatures in significant numbers and, since they are considered as mobile species, they contribute to defect recombination with vacancies, and therefore I_2Cr clusters affect defect evolution. It is not clear from the results presented above if higher order clusters also have an important influence in the simulation results in terms of recovery of the resistivity. In order to understand the importance of clusters with more than one Cr atom we have eliminated from the simulations the formation of ICr_2 and I_2Cr_2 clusters, and repeated the calculations for all three Cr concentrations. Fig. 5 shows the derivative of the normalized defects with temperature for the case of the highest Cr concentration, 0.095 at.%, both when these reactions are included and when they are excluded from the calculation. The case of pure Fe is also shown in Fig. 5 for comparison. It is clear from this figure that, at least for the temperature range considered, these clusters have a small impact on the defect evolution. The reason for such behavior is the low dissociation energy of these clusters; ICr_2 dissociates into Cr and ICr with a barrier of 0.31 eV, while I_2Cr_2 dissociates into Cr + I_2Cr with a barrier of 0.36 eV. Therefore, at the temperatures at which these defects are formed, the dissociation is also very likely. The growth

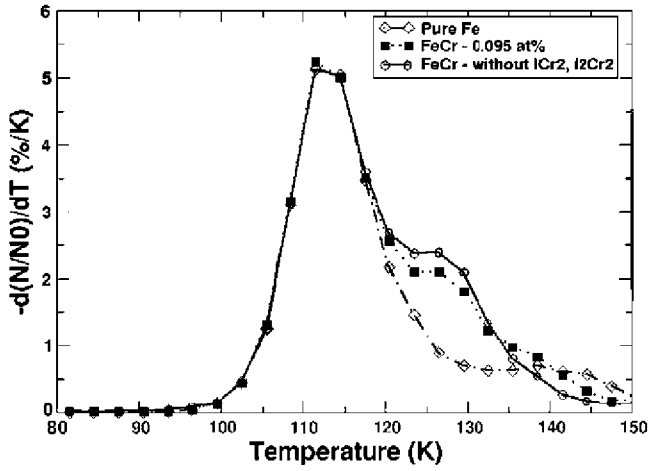

Fig. 5. I_{D2} and I_E peaks with and without ICr_2 and I_2Cr_2 clusters for a Fe–Cr alloy with 0.095 at.% of Cr.

of higher order Cr clusters (more than two Cr atoms) could occur by the interaction of the mobile ICr and I_2Cr complexes if the stability of such I_nCr_m clusters is high enough.

4. Conclusions

We have performed OKMC simulations of the isochronal annealing of electron irradiated Fe and dilute Fe–Cr alloys to compare our results with resistivity recovery measurements of Abe and Kuramoto [5]. The OKMC model used parameters obtained from DFT calculations and interatomic potentials of different sources [9–11]. The model is able to reproduce the shift of the peak corresponding to the I_E stage with Cr concentration observed experimentally, and explains this shift by the formation of mixed Fe–Cr dumbbells which have a lower migration energy than Fe self-interstitials, as was originally proposed by Maury et al. [14]. These calculations have also shown the importance of the choice of the capture radius for the interaction between a substitutional Cr and self-interstitial Fe. A small capture radius, of the order of the lattice parameter, a_0, must be considered in order to reproduce the experimental observations. Finally, the influence of clusters with high Cr content on defect evolution has been evaluated. We have observed that below 150 K, a simplified model where ICr_2 and I_2Cr_2 complexes are not included in the calculation, also provides a good agreement with the experimental measurements of resistivity recovery.

Acknowledgements

We thank C. Ortiz, L. Malerba and M. Victoria for fruitful discussions. This work was supported by the FPVII project FeMAS, the FPVII project GETMAT and the MAT-REMEV task of EFDA.

References

[1] L. Malerba, A. Caro, J. Wallenius, J. Nucl. Mater. 382 (2008) 112.
[2] S.L. Dudarev, J.-L. Boutard, R. Lässer, M.J. Caturla, P.M. Derlet, M. Fivel, C.-C. Fu, M.Y. Lavrentiev, L. Malerba, M. Mrovec, D. Nguyen-Manh, K. Nordlund, M. Perlado, R. Schäublin, H. Van Swygenhoven, D. Terentyev, J. Wallenius, D. Weygand, F. Willaime, J. Nucl. Mater. 386–388 (2009) 1.
[3] R. Andreani, E. Diegele, W. Gulden, R. Lässer, D. Maisonnier, D. Murdoch, M. Pick, Y. Poitevin, Fus. Eng. Design 81 (2006) 25.
[4] B. van der Schaaf, E. Diegele, R. Laesser, A. Moeslang, Fus. Eng. Design 81 (2006) 893.
[5] H. Abe, E. Kuramoto, J. Nucl. Mater. 271–272 (1999) 209–213.
[6] M.H. Kalos, P.A. Whitlock, Monte Carlo Methods, vol. 1, John Wiley & sons, 1986. Basics.
[7] M.D. Johnson, M.-J. Caturla, R. Diaz de la Rubia, J. Appl. Phys. 84 (1998) 1963.
[8] C. Ortiz, M.J. Caturla, Phys. Rev. B 75 (2007) 184101.
[9] P. Olsson, J. Nucl. Mater. 386–388 (2009) 86.
[10] D. Terentyev, N. Castin, Comp. Mat. Sci. 46 (2009) 1178.
[11] C.C. Fu, J. Dalla Torre, F. Willaime, J.-L. Bouquet, A. Barbu, Nat. Mater. (2004).
[12] F. Maury, M. Biget, P. Vajda, A. Lucasson, P. Lucasson, Phys. Rev. B 14 (1976) 5303.
[13] S. Takaki, J. Fuss, H. Kugler, U. Dedek, H. Schultz, Radiat. Eff. 79 (1983) 87.
[14] F. Maury, P. Lucasson, A. Lucasson, F. Faudot, J. Bigot, J. Phys. F: Met. Phys. 17 (1987) 1143.
[15] C. Ortiz, D. Terentyev, J. Nucl. Mater. (in press).
[16] P. Olsson, C. Domain, J. Wallenius, Phys. Rev. B 75 (2007) 014110.
[17] D. Terentyev, P. Olsson, T.P.C. Klaver, L. Malerba, Comp. Mat. Sci. 43 (2008) 1183.